Misan Journal of Engineering Sciences ISSN-E: 2957-4250
Vol. 4, No. 2, Dec 2025 ISSN: 2957-4242

A Study of Hybrid Aluminum Base Alloy for Bending Fatigue Resistance

Jasim H. AL-Bedhany [*,1], Ali Hussein Al-azzawi [2]

[1*] *University of Misan, Engineering College, Mechanical Eng. Dept.; Iraq*
[2]*University of Misan, Engineering College, Chemical Eng. Dept.; Iraq*
**Corresponding author E-mail: j.h.al-bedhany@uomisan.edu.iq*
(Received 20 July, Revised 28 July, Accepted 29 July)

Abstract: Using of aluminum and aluminum base are widely used for mechanical components. Hybrid aluminum base alloys are type of alloys with composition differs from the standard percentages. The use of these alloys instead of steel alloys have increasing expansion due to their low weight to toughness ratio and their superior mechanical properties. Fatigue resistance is one of the important properties due exerting most of the mechanical components to cyclic and variable loadings. In this study a hybrid aluminum base alloy has a compositions (Aluminum 85%, Silicon 10% and Chrome5%) is used to investigate its mechanical properties and fatigue resistance under constant completely reversed cyclic loadings under bending rotation.

The results identified a relatively poor bending fatigue resistance under low fatigue regime, with relatively long fatigue life under low bending loading compared with the other hybrid aluminum base alloys with average bending stress*fatigue life of (214,5392 MPa. cycle). The results also confirm the applicability of AL-Bedhany Energy Fraction of Damage Accumulation (EFDA) fatigue damage theory, which depends on the area under S-N curve under the average loading level in MPa cycle. The percentages of errors between 8.7% to -20.5% for the predicted fatigue life according to the gradual propagation of the fatigue cracks of this alloy appears clearly at the fracture regions due to alloy' malleability. This makes this alloy suitable only for manufacturing the shafts with relatively low bending stress.

Keywords: Aluminum base alloy, fatigue life prediction, EFDA, bending fatigue, fracture morphology

1. Introduction

Using of aluminum base alloys to manufacturing blades to produce airplanes' bodies; however, small shafts especially for the mechanical constructions which requires low weights make the aluminum base alloys may be one of the important replacement to the steel shafts. For these, a considerable number of studies have been conducted to specify the important mechanical properties for different alloys with aluminum base. Steel alloys' fatigue life usually have a long fatigue life (High Cycle Fatigue (HCF) regime) with many millions of fatigue cycles to be suitable for applications.

DOI: https://doi.org/10.61263/mjes.v4i2.191

Tobushi et al. [1] studied the cyclic deformation of a TiNi alloy wire using rotating-bending fatigue at various rates of strains under different temperature levels in media of water and air. Their results showed the amplitude of strain in the phase transformation region where the fatigue life was longer and the properties of deformation did not change under cyclic strain; also, the cyclic life was shorter with elevating the temperature. They also concluded that, the rotational speed does not affect the actual life in water but being higher in air. On the other hand; Hesami *et al.* [2] investigated a one-dimensional model to study the rotary bending cyclic fatigue in beams made from TiNi alloy. The distributions of strain and stress in the beam section using numerical technique for two cases with pure and rotary bending to study the differences between these two loadings. Their results verified using experimental procedure. Since the test specimens exposed to reversed transformation of stress–strain response, an innovated stress–temperature diagram was proposed with different slopes for the start and finish for the test specimen. The test results controlled by a power law for the variations of the fatigue life using dissipated energy to estimate the fatigue life. The results showed a good agreement with the experimental findings. The results also verified by the uniaxial tensile fatigue tests which conducted to study the effect of loading type on the cyclic life.

Lai et al. [3] investigated the cyclic fatigue properties of C17200 alloy on a quenching aging heat treatment under high temperatures to study the application under certain range of temperatures. Tensile and rotary bending fatigue tests have been carried out at the temperatures of 25C^{o}, 150C^{o}, 350C^{o}, and 450C^{o}). The relationships between the bending stress and the number of cycles to failure were fitted as S-N curves. The observation of the fractured surfaces were analyzed by a Scanning Electron Microscopy (SEM). Their results clarified the performance of rotating bending fatigue, when the temperature reaches 450 C^{o}. the fatigue failure type of the alloy belongs to be surface initiated as defects. Below 350 C^{o}, the failed surfaces seem to have a brittle fracture behavior. On the other hand Almaraz et al. [4] studied the rotating bending fatigue using experimental tests on aluminum alloy 6061-T6. The test loading conditions were close to the material elastic limit. Artificial pitting has been introduced in several specimens to compare with the case of no pitting. Their results showed that the endurance is reduced in the case of increasing the pitting holes. The numerical analysis using FE also conducted to determine the stress concentrations. The stress concentration for two or more pitting holes have been considered for the analysis of the application of fatigue life prediction under corrosion attack. Almaraz et al. in another study [5], investigated the rotating bending fatigue for aluminum alloy 6063-T5 with pre-corroded and non-corroded specimens by immersion of specimens in an acid solution of hydrochloric acid with a concentration of 38% for two to six minutes to achieve three levels of corrosion. The reduction of fatigue endurance can be controlled by the surface corrosion of the testing specimens. Additionally, the investigation of numerical crack propagation was carried out for the testing specimen and using the Displacements Correlation Method (DCM). The conclusions showed concerning the rotating bending fatigue where, the crack propagation and the behavior of fatigue-corrosion for this material.

Behvar and Haghshenas [6] studied The increase in temperature as a cause of premature fatigue failure. As a state-of-the-art review paper, they focused on fatigue life and microstructural models. Their results specified the demand of using microstructural characterization in the fatigue life models since the additive to manufacture the alloys and the induced processing defects add several difficulties on explaining the fatigue modeling. They also conclude the necessity for a multidisciplinary approach by integrates the mechanics, materials science, and data science to optimize the materials fatigue loadings and the fatigue life.

The effect of surface coating by anodizing. have been investigated by Nakamura et al. [7] by studying the coating by oxide layer which widely used as a surface coating for aluminum alloy due to its high wear resistance, high hardness, and electrical resistance that reflected on the fatigue behavior. Many fatigue tests have been carried out on several samples of aluminum alloy using a dual-spindle machine to apply rotating bending fatigue testing. The results compared with untreated specimens by examining the failed samples using Scanning Electronic Microscope (SEM), by evaluating the fractography and fracture mechanics. Their results showed that, for low cyclic fatigue regime, a significant deteriorations of the fatigue strength in comparison with the untreated specimen. However, for (more than 100 million cycles), the fatigue strength becomes a little higher than the untreated specimen.

The applications of the aluminum base alloy are widely spread in different applications; however, this research focus on the practical engineering applications. Minto et al. [8], investigated the association of structural fatigue with the surface damage using AA 7050-T7451 aluminum alloy. The enhance of performance by insulating and reducing the environmental impact on aircraft body probably enhance the fatigue life. Their results showed the different surface processes have various effects on improving the fatigue life (negative and positive impacts).The aims of the experimental works of their investigations are to study the effect of plasma immersion ion implantation (PIII) on the fatigue life under rotating and bending fatigue. The results showed that the implantation of low impact frequency increased the fatigue life and enhanced the roughness without decrease in the base material' micro-hardness of the base material; however, for high impact frequency the fatigue life reduced.

The effects of strontium addition and heat treating both in isolated and combined forms on the fatigue life have been studied by Haskel and. Barbieri [9] using A356 alloy and bending fatigue tests. Additionally, the micro-hardness and tensile tests have been used to study the microstructural characterization and fracture of the surface. They showed a direct relationship between the cyclic and static properties. The results indicated that with T6 condition of heat treatment and low cycle fatigue, the test samples showed the best behavior, with slightly lower performance in low cycle ($N \cong 2\times10^6$ cycles). Their observations of fracture analysis, showed changes in the morphology of the silicon particles in the fracture mode. Their findings also indicated that, at T6 conditions A356 alloys showed a modified fatigue life in Low Cycle Fatigue (LCF) compared with the High Cycle Fatigue (HCF) without significant modification in the fatigue strength.

Mobark et al. [10] performed a comparative investigation of the microstructural characteristics and tribological behavior of two different aluminum base alloys,. The tribology analysis have been conducted to assess wear resistance, crack formation and propagation, and the cavity zones by using optical and SEM microscopes. Their results showed significant differences between the

investigated two alloys, and the alloy with 77.3% Al, 1.8% Fe and 16.7% Si showed a higher Vickers hardness and a noticeable wear resistance modification compared to the 54.1% Al, 12.8% Fe and 27.8% Cr alloy. Al-Azzawi et al. [11] also studied another alloy with different compostion to assess wear and crack formation, Their results showed that, the specimens exhibit higher Vickers hardness and superior wear resistance.

In summarize, the majority of the previous works focused on using blades under tensile loading; studying the reverse loading with cylindrical test specimens will give a clearer view to investigate the fatigue behavior and the possibility of using aluminum base hybrid alloys to manufacture shafts and the other mechanical components under completely reversed loading. The purpose of this research within the real-world enginnering. This study uses cylindrical test specimen to investigate the fatigue behavior of a suggested composition alloy.

2. Theoretical stress calculations

2.1 Stress calculation

Rotating bending fatigue depends on introducing a bending stress on a standard specimen. The general law of bending stress can be written as [12]:

$$\frac{\sigma}{Y} = \frac{BM.}{I} \tag{1}$$

Where, σ is the bending stress, BM. is the bending moment applied on the specimen, Y is the maximum distance from the cross-section centerline and I, is the area moment of inertia of the cross-section of the test sample at the neck region. Equation (1) can be re-written as: (See Figure 1).

$$\sigma = \frac{BM.Y}{I} \tag{2}$$

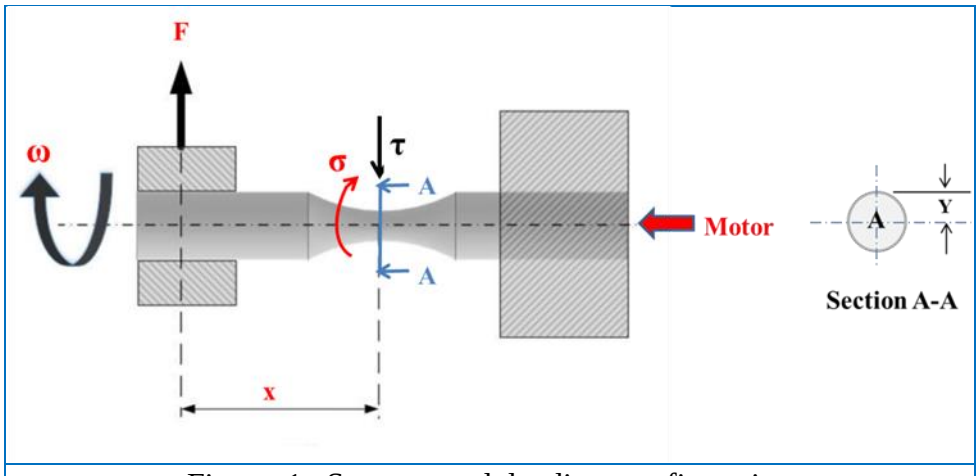

Figure 1. Stresses and loading configuration

Shear stress (τ) also introduced at the Section A-A in Figure 1, which can be calculated as:

$$\tau = \frac{F}{A} \tag{3}$$

Where F is the applied force and A is the cross-sectional area. Because the shear stress is small compared with the bending stress; some studies neglect the shear stress but, not in this study. The resultant (maximum principal stress (σ_1) can be calculated as:

$$\sigma_1 = \sqrt{\sigma^2 + \tau^2} \quad (4)$$

Figure 1, also shows the required dimensions and force to calculate the bending moment;

$$BM. = F * x \quad (5)$$

2.2 Test specimen dimensions

The rotating bending fatigue tests, used to evaluate the fatigue life of the materials behavior under cyclic bending stresses, are standardized by several organizations, most notably ISO 1143 [13]. This standard outlines the procedures for conducting these tests, including specimen preparation, machine setup, and data analysis. The dimensions of one of the rotating bending fatigue specimen can be seen in Figure 2.

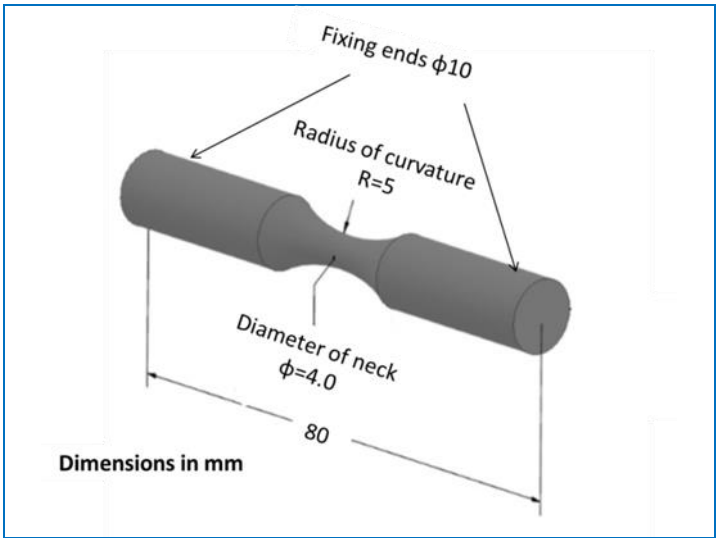

Figure 2. Dimensions of the test specimen

For the dimensions shown above in Figure 1, the length (x in Eqn5) is 40 mm i.e, x= 0.04 m (a half of the test specimen length). The hanging weights (the load) are 1 to 4.5 kg with 0.5 kg step as illustrated in Table 1. This table also illustrated the required calculations including the principal stress.

Table 1. Stresses due to hanging the testing weights

Weight (kg)	BM. (N.m)	Bending stress (MPa)	Shear stress (MPa)	Principal stress (MPa)
1.0	0.3924	62.427	0.780	62.432
1.5	0.5886	93.641	1.171	93.648
2.0	0.7848	124.855	1.561	124.864
2.5	0.981	156.068	1.951	156.080
3.0	1.1772	187.282	2.341	187.296
3.5	1.3734	218.495	2.731	218.513
4.0	1.5696	249.709	3.121	249.729
4.5	1.7658	280.923	3.512	280.945

3. Experimental works

The procedure of casting and preparing the test samples will be briefly explained, then the plan of tests loading data will be detailed.

3.1 Alloy and sample preparation

The main objective of this study is evaluating the mechanical properties, especially the fatigue resistance of a hybrid aluminum alloy with specific compositions as illustrated in Figure 3. Each component (material) has been weighted using a four-digit balance before melting in a gas furnace and mixing with hot plate stirrer mixer. The melted mixing alloy material have been casted in a sand die to get approximately a cylindrical shape, which machined using lathe machine. The final stage of sample preparation consists of the grinding and polishing stage to have a surface roughness (Ra= ~0.2 µm) to coincide with the test standard. The surface roughness has been checked using a linear surface roughness profilometer with ability to make a radius compensation type MITUTOYO®SJ.40. The samples then tested using rotating bending fatigue machine.

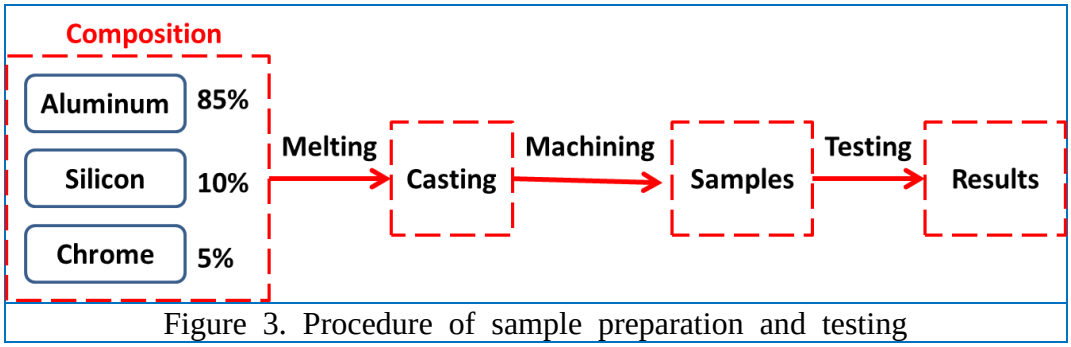

Figure 3. Procedure of sample preparation and testing

To check the uniform distribution of the alloy contents, several images have been taken using optical microscope as can be seen in Figure 4. The microstructure of the alloy was uniform with normal inclusions (~5 µm length) and small voids adjacent to the inclusion boundaries.

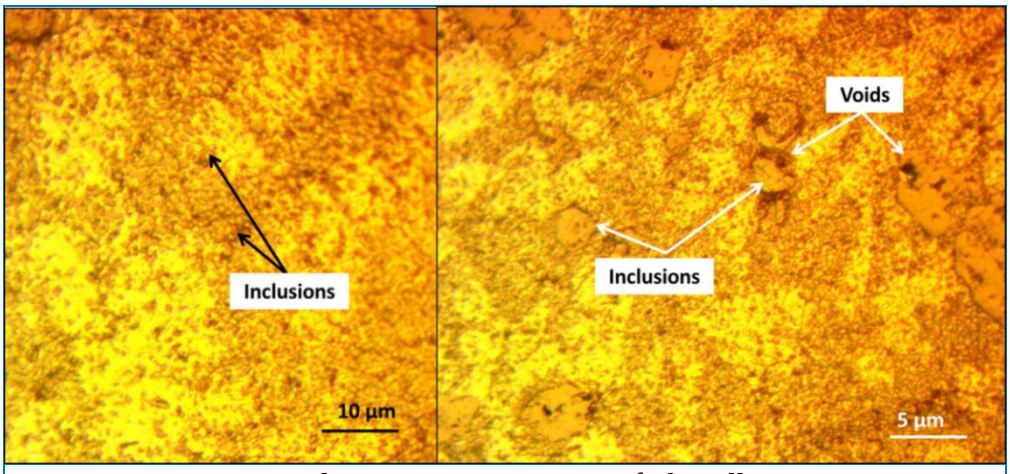

Figure 4. Two optical microscope images of the alloy microstructure

3.2 Fatigue tests

The fatigue-testing machine presenting in Figure 5, has been used to conduct the rotating bending fatigue tests. The hanging weights by the loading rob over a free rotating pulley can applied the same weights on the other side of the pulley, which transferred to introduce the bending on the test specimens. The rotating specimen takes its rotational movement from an AC 1.5 HP motor via a shaft consisting of a counter sensor to count the number of cycles and present the cycles number on a digital screen. The test frequency has been adjusted at 25 Hz (1500 rpm) by controlling the motor speed.

Eight weights have been chosen to conduct the required tests within the range of 1 kg to 4.5 kg by 0.5 kg of loading step as illustrated in Table 2. To increase the reliability; each test has been repeated three times and the average has been calculated and considered. The percentage of error (deviation of the test No. of cycles) also calculated and presented in the same table. Eqn. 6 used to calculate the error percentage as:

$$Error\ \% = \frac{Test\ No.of\ cycles - average\ No.of\ cycles\ under\ the\ load}{Average\ No.of\ cycles\ at\ the\ load} X\ 100\% \quad (6)$$

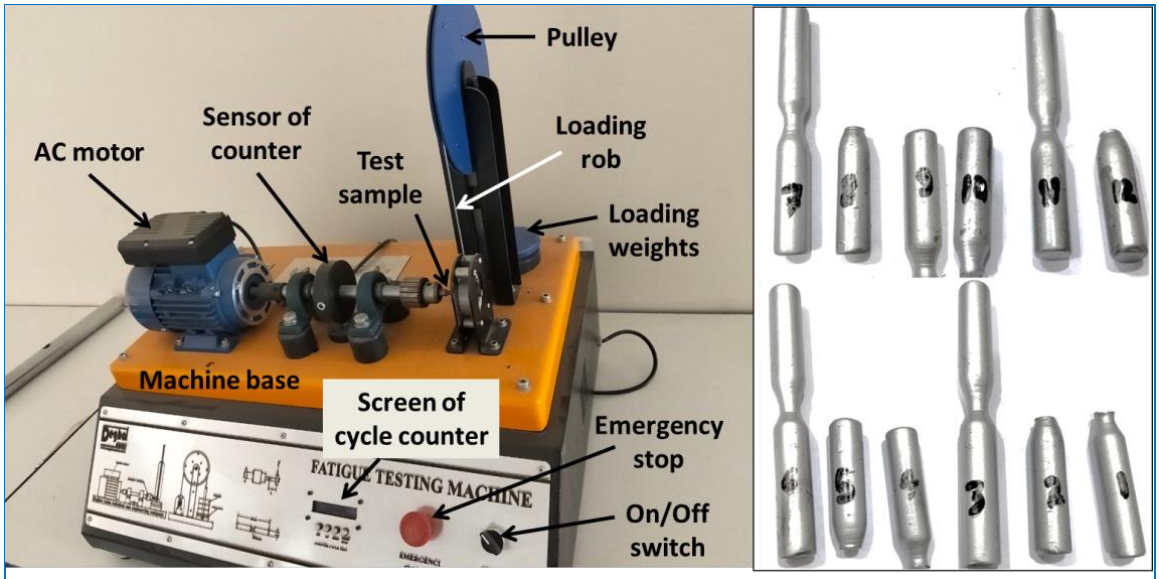

Figure 5. Details of the fatigue testing machine and test samples

Table 2. Experimental results of fatigue tests with errors

Weight (kg)	No. of cycles to failure				Max. Negative Error %	Max. Positive Error %
	Test 1	Test 2	Test 3	Average		
1.0	30017	35219	31286	32174	-7	9.5
1.5	18945	17552	20122	18873	-7	6.6
2.0	19158	15403	17265	17275	-11	10.9
2.5	11382	14106	14827	13438	-15	10.3
3.0	11072	9844	7763	9559	-5	9.2
3.5	8756	12058	10389	10401	-16	15.9
4.0	10054	9433	7055	8847	-17	13.6
4.5	5519	7225	6158	6300	-12	14.7

4. Results

4.1 Fatigue life tests

Presenting the data achieved from the fatigue tests in Figure 6. showing noticeable trend of the stress/Number of cycles to failure curves (S-N curves). Despite the relatively significant scatter in the fatigue test results (which is normal in fatigue tests), and the relatively high percentages of errors between -17% to +15.9%. The trend curves being close to each other under relatively high stress bending fatigue tests; however, under low stress the trend curves separate.

The percentages of error vary randomly by increasing and decreasing without any relevant with the fatigue test load and life.

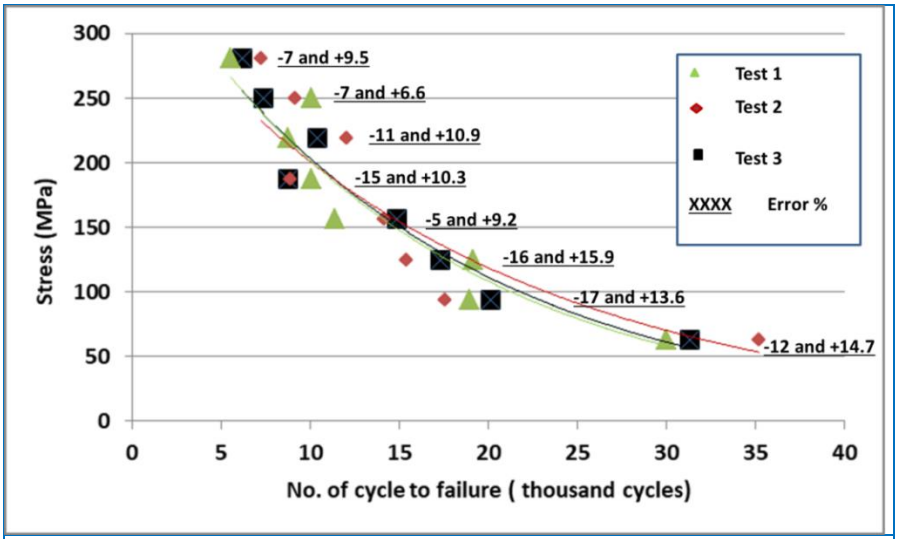

Figure 6. Fatigue life results of the conducted tests

4.2 Microscopic examination

Optical microscope has been used to investigate the morphology of the fracture regions. The fracture zone appears shining under optical light; that pushed towards using dark mode in the microscope and uncolored images to increase the resolution of the examine regions as can be seen in Figure 7. The general examine of the fractography showing at least two distinguished regions within fracture region of each test sample. The cracks having the largest lengths are associated with the external surface of the testsample. This confirms the surface crack initiation i.e. the fracture in rotating bending fatigue initiates from the surface. Subsurface microcracks also observed within the distinguished fracture regions.

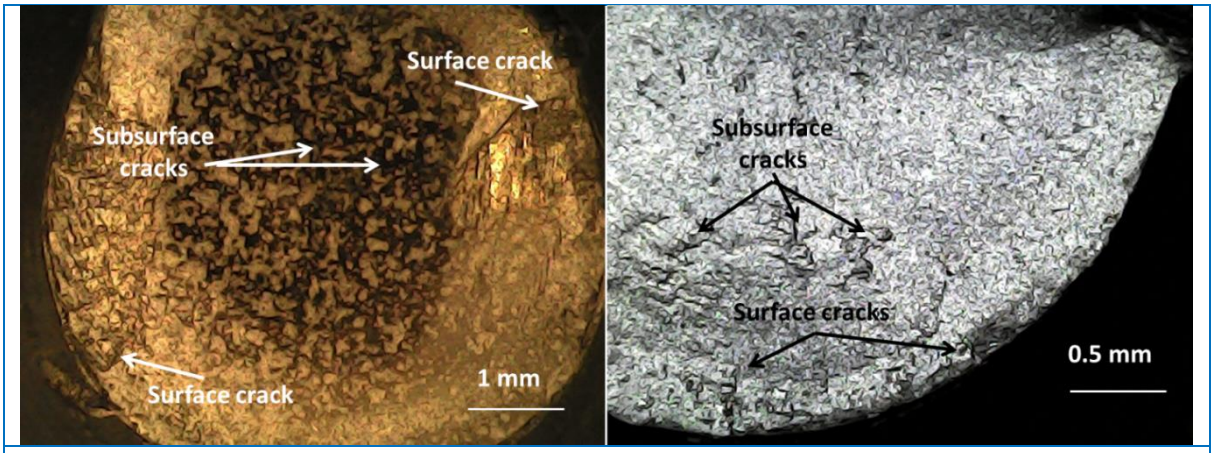

Figure 7. General microscopic examination of the fracture region for two test samples under 4 kg loading.

Investigating other test samples confirms the surface crack initiation. Figure 8 shows another two test samples; a significant expansion of the surface cracks towards the center of rotation has been observed. The observed subsurface microcracks seem to have expansion in different directions.

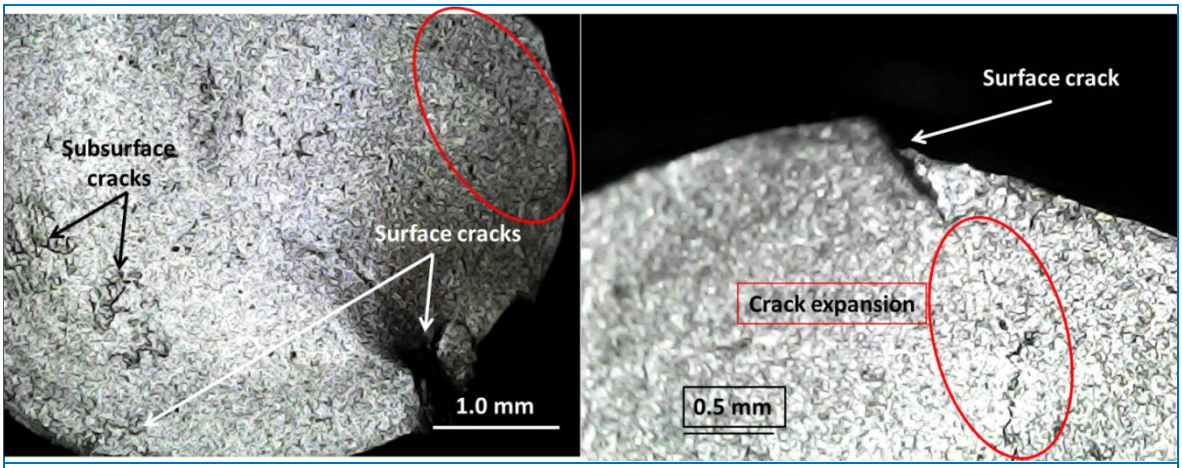

Figure 8. Expansion of surface and subsurface cracks under 2.5 kg (left) and 3.5 k g (right) loading levels

The fine black spots within the samples represent inclusions and casting small voids within the sample' material. Each test sample has different distinguished fracture areas with different morphologies labeled A, B and C in Figure 9. The width (radial distance) of the fracture regions approximately equals for the tests under the same loading and rotating speed i.e. repeated tests. For other tests, these regions being narrower with increasing the testing load (since the test frequency was constant).

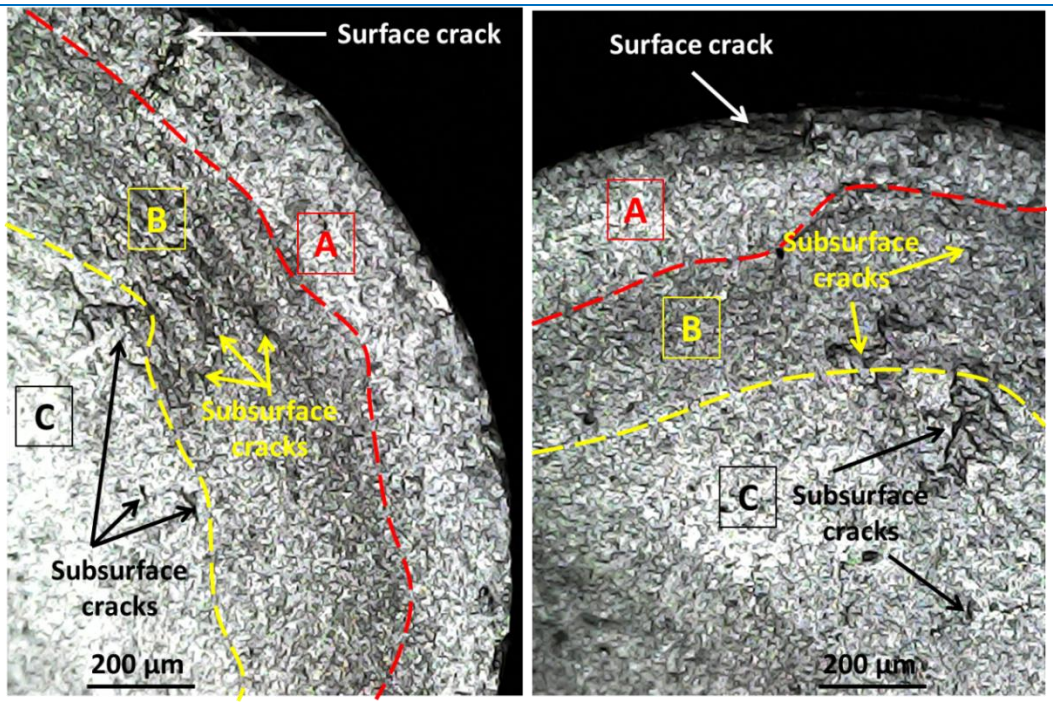

Figure 9. Fracture regions of two test samples unser 1.5 kg (left) and 4.5 kg (right) loading levels

Focusing on the transient regions (the locations between two sequential fracture morphologies), showing a considerable number of microcracks in circumferential direction; however, within these regions, the cracks have random directions as can be seen in Figure 10.

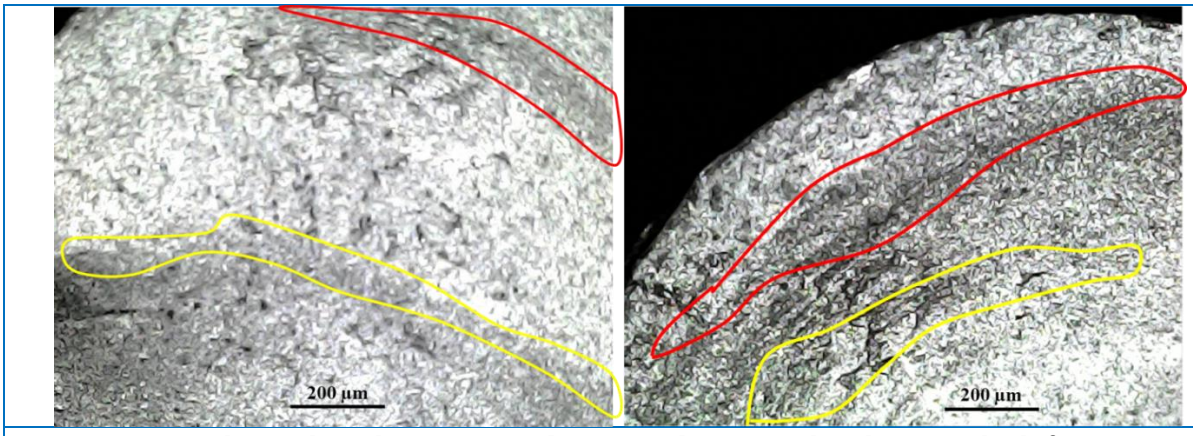

Figure 10. Cracks within the transient locations between the distinguished fracture zones under 3.0 kg (right) and 4 kg (left) loading levels.

4.3 Energy Fraction of Damage Accumulation (EFDA) method

Presenting the average fatigue life for every loading level illustrated in Table 2 with the calculated principal stress in Table 1 gives the S-N of the alloy which can be seen in Figure 11. The error residue of the exponential trend curve shows a deviation from the average curve

(error) with ~7.3%. The average loading level can be easily calculated (2.75 kg) with its corresponding stress (171.7 MPa) and the fatigue life can be found from the horizontal axis of the achieved S-N curve (12,495 cycle) as presented with red lines.

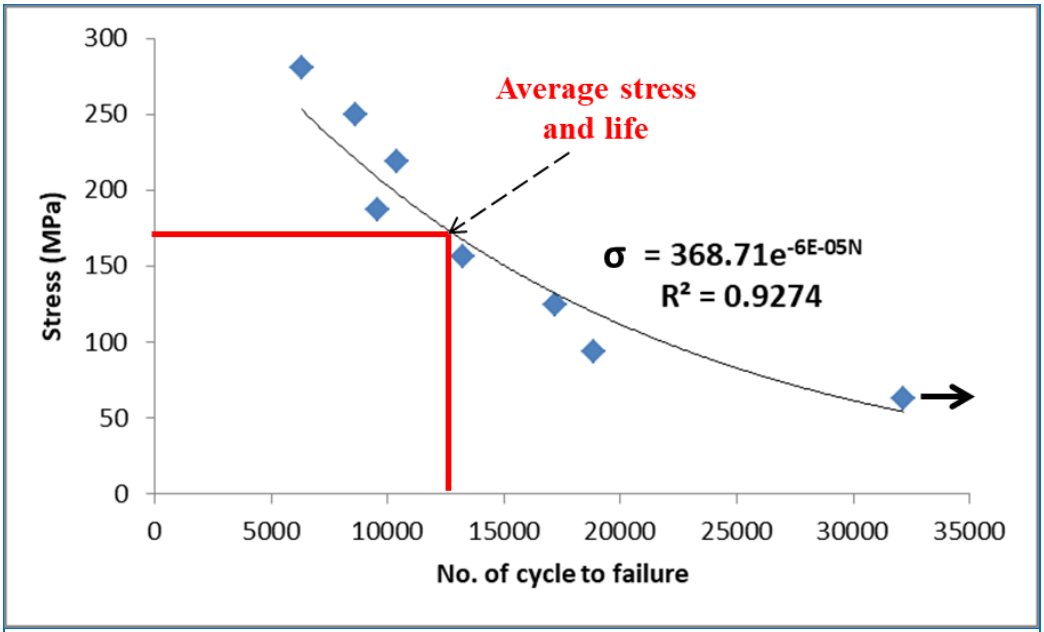

Figure 11. S-N curve of the average results for the test material

AL-Bedhany et al. [14], proposed a new theory of fatigue damage named Energy Fraction of Damage Accumulation (EFDA) (more details can be found in Reference [15]. This theory depends on the area under S-N curve measured in MPa.cycle under the average loading level, then, predicting the bfatigue life under other loading level by equating the area under the average loading level with that of the selected level. This section will test the applicability of this theory on the conducted tests. The method depends on calculating the area under S-N curve at the average loading level and using this area to predict the fatigue life under any other stress level. The area for the achieved S-N curve is (171.7*12,495 = 214,5392 MPa.cycle).

The y-function (trend curve) in Figure 11 can be used to calculate the stress (σ) as a function of the number of cycles to failure (N). In practical case; at a given stress level, the predicted fatigue life should be calculated thus, the given equation should be changed to find the number of cycles (N) as a function of the known stress loading level (σ). The equation will be:

$$N = 39602\, e^{-0.007\sigma} \tag{7}$$

Where, N is the number of cycle to failure and σ is the principal stress due to bending. The area under the S-N curve for the every actual experimental fatigue test and the predicted fatigue life using the trend curve have been calculated and illustrated in Table 3. The percentage of errors between the actual and predicted life according to EFDA theory have been calculated and presented in this table. The percentage of errors between the predicted life with the life can be achieved from the calculation depending on the trend curve.

Table 3. EFDA method and its error for the tests.

stress (Mpa)	Actual Average No. of cycle to failure	Area under S-N curve (Mpa. cycle)	Error %	Predicted No. of cycle to failure using average S-N curve	Error %
171.7	12495	2145391.5	Reference predicted test		
62.4322	32163	2008020	-6.40	25581	-20.46
93.6482	18869	1767057.6	-12.00	20560	8.96
124.864	17207	2148581.4	21.59	16524	-3.97
156.080	13251	2068260.6	-3.74	13281	0.22
187.296	9541	1787137.8	-13.59	10674	11.87
218.513	10384	2269062.6	26.97	8579	-17.39
249.729	8603	2148581.4	-5.31	6895	-19.86
280.945	6290	1767057.6	-17.76	5542	-11.90

5. Discussions

There were 24 tests (three groups with 8 testing levels) have been conducted to get the mechanical properties of aluminum base alloy. Fatigue resistance of this alloy and S-N curve have been performed. The bending rotating fatigue testing results showed a low fatigue cycle regime is the general behavior of this alloy and the unsuitability of using this alloy to manufacture shafts instead of steel and its alloy. The repeating of a test under the same loading conditions gives different fatigue lives. The trend lines of each testing group (under different loading levels) were close to each other under high loading levels (shorter fatigue lives); however, under low loading levels (longer lives), the trend lines separated. This behavior confirms the increasing of error percentages under low loading levels. The microstructural investigation showed at least two distinguished morphologies of the fracture surfaces and these topographies approximately having equal radial widths for the tests under the same loading levels (repeated tests). For low loading levels (longer fatigue lives); the number of these distinguished topographies increased and having narrower radial widths.

EFDA theory of fatigue life prediction can be used to predict the rotating bending fatigue life depending on the average loading levels with acceptable percentages of error (less than 12%); however, two singular tests (highlighted in Table 3) have been observed for the comparison of actual fatigue lives with the predicted one using this theory. These singular results probably due to the microstructural differences i.e. distribution of impurities (inclusions and voids) within the fractured surfaces. When using the trend curves of average S-N curve; the percentages of error usually less than 20%. The majority of error percentages were with negative values i.e. the predicted life often less than the actual life and this a good sign to prepare for the fracture before its happening.

6. Conclusions

According to the previous discussion and the presented results; the following conclusions can be drawn:

- For the alloy base with the specified compositions and testing loading levels, the general fatigue behavior was low cycle fatigue and this showed the unsuitability of manufacturing shafts from this alloy instead of steel alloys even under relatively low loading stress levels.
- The fractography of the failed surfaces consists of more than two distinguished topographies and the number of these distinguished areas increased and being narrower with decreasing the test loading (for relatively longer fatigue lives).
- The fatigue failure is surface initiated and there are several subsurface fatigue cracks in circumferential direction have been observed for all the tests and these cracks concentrated at the interfaces between every two sequential distinguished topographies of the fracture surfaces. These cracks probably introduced in a plane close to the fracture plane and they pass at the fracture surface throughout the crack propagation stage.
- EFDA theory can predict less fatigue lives for rotating bending fatigue for the actual (experimental) fatigue between -3.74 to -17.76 with a possibility of 12.5 % of wrong prediction (2 from 8 tests highlighted in Table 3).

Acknowledgements

The researcher would like to thank and express the deepest gratitude grateful to every one of the construction laboratories at the Mechanical Engineering Dept. , Engineering college, University of Misan for their help and support.

Author Contributions: The authors contributed to all parts of the current study.
Funding: This study received no external funding.
Conflicts of Interest: The authors declare that no conflict of interest with any external parties is found.

References

[1] H. Tobushi, T. Hachisuka, T. Hashimoto, and S. Yamada, “Cyclic deformation and fatigue of a tini shape-memory alloy wire subjected to rotating-bending,” *Proc. ASME Des. Eng. Tech. Conf.*, vol. 1B-1997, no. January 1998, 1997.

[2] M. Hesami *et al.*, “Rotary bending fatigue analysis of shape memory alloys,” *J. Intell. Mater. Syst. Struct.*, vol. 29, no. 6, pp. 1183–1195, 2018.

[3] F. Lai, K. Mao, C. Cao, A. Hu, J. Tu, and Y. Lin, “Rotating Bending Fatigue Behaviors of C17200 Beryllium Copper Alloy at High Temperatures,” *Materials (Basel).*, vol. 16, no. 2, 2023.

[4] G. M. Dominguez Almaraz, V. H. Mercado Lemus, and J. Jesús Villalon Lopez, “Rotating bending fatigue tests for aluminum alloy 6061-T6, close to elastic limit and with artificial pitting holes,” *Procedia Eng.*, vol. 2, no. 1, pp. 805–813, 2010.

[5] G. M. Domínguez-Almaraz, J. L. Ávila-Ambriz, F. Peyraut, and E. Cadenas-Calderón, "Effect of controlled corrosion attack with HCl acid on the fatigue endurance of aluminum alloy AISI 6063-T5, under rotating bending fatigue tests," *Mater. Res. Soc. Symp. Proc.*, vol. 1485, pp. 53–58, 2013.

[6] A. Behvar, F. Berto, and M. Haghshenas, "A review on isothermal rotating bending fatigue failure: Microstructural and lifetime modeling of wrought and additive manufactured alloys," *Fatigue Fract. Eng. Mater. Struct.*, vol. 46, no. 10, pp. 3545–3595, 2023.

[7] Y. Nakamura, T. Sakai, H. Hirano, and K. S. Ravi Chandran, "Effect of alumite surface treatments on long-life fatigue behavior of a cast aluminum in rotating bending," *Int. J. Fatigue*, vol. 32, no. 3, pp. 621–626, 2010.

[8] T. A. Minto, V. M. C. A. de Oliveira, and H. J. C. Voorwald, "Plasma immersion ion implantation: Influence on the rotating bending fatigue strength of AA 7050-T7451 aluminum alloy," *Int. J. Fatigue*, vol. 103, pp. 17–27, 2017.

[9] T. Haskel, G. O. Verran, and R. Barbieri, "Rotating and bending fatigue behavior of A356 aluminum alloy: Effects of strontium addition and T6 heat treatment," *Int. J. Fatigue*, vol. 114, pp. 1–10, 2018.

[10] H. F. H. Mobark, A. H. Al-Azzawi, A. K. AbidAli, and B. Mohamad, "COMPARATIVE TRIBOLOGICAL ANALYSIS OF Al-Fe-Si AND Al-Fe-Cr BASED ALLOYS UPOREDNA TRIBOLOŠKA ANALIZA LEGURA TIPA Al-Fe-Si I Al-Fe-Cr," *Struct. Integr. Life*, vol. 24, no. 3, pp. 386–392, 2024.

[11] H. F. H. Mobark, A. H. Al-Azzawi, M. T. M. F. Agha, A. K. A. Ali, and B. Mohamad, "Comparative Tribological Analysis of Al–Fe–Si-Based Alloys," *Metallofiz. i Noveishie Tekhnologii*, vol. 46, no. 10, pp. 991–1005, 2024.

[12] E. J. Hearn, "Mechanics of," no. January 2001.

[13] BS ISO 1143:2021, "Metallic materials-Rotating bar bending fatigue testing Matériaux métalliques-Essais de fatigue par flexion rotative de barreaux," vol. 2021, 2021.

[14] J. AL-Bedhany, S. LEGUTKO, A. AL-Maliki, and T. A. Mankhi, "A New Theory of Damage Estimation and Fatigue Life Prediction," *Misan J. Eng. Sci.*, vol. 2, no. 2, pp. 1–11, 2023.

[15] J. H. I. AL-Bedhany, "Effect of Compression, Impact and Slipping on Rolling Contact Fatigue and Subsurface Microstructural Damage," no. February, 2020.